Published in final edited form as:
FEBS J. 2011 February ; 278(4): 643–653. doi:10.1111/j.1742-4658.2010.07985.x.

Roles of the SH2 and SH3 domains in the regulation of neuronal Src kinase functions

Bradley R. Groveman[1], **Sheng Xue**[2], **Vedrana Marin**[1], **Jindong Xu**[2], **Mohammad K. Ali**[1], **Ewa A. Bienkiewicz**[1], and **Xian-Min Yu**[1,2]

[1] Department of Biomedical Sciences, College of Medicine, Florida State University, Tallahassee FL 32306-4300, USA

[2] Faculty of Dentistry, University of Toronto, Ontario M5G 1G6, Canada

Abstract

Previous studies demonstrate that intradomain interactions of Src family kinases (SFKs), stabilized by binding of the phosphorylated C-tail to the SH2 domain and/or the binding of the SH2-kinase linker to the SH3 domain, lock the molecules in a closed conformation, disrupt the kinase active site and inactivate SFKs. Here we report that the up-regulation of N-methyl-D-aspartate receptors (NMDARs) induced by expression of constitutively active neuronal Src in which the C-tail tyrosine is mutated to phenylalanine (n-Src/Y535F) is significantly reduced by dysfunctions of the SH2 and/or SH3 domains of the protein. Furthermore, we found that the dysfunctions of SH2 and/or SH3 domains reduce the autophosphorylation of the kinase activation loop, depress the kinase activity, and decrease NMDAR phosphorylation. The SH2 domain plays a greater regulatory role than the SH3 domain. Our data also show that n-Src binds directly to the C-tail protein of the NMDA NR2A subunit *in-vitro* with a K_D of 108.2 (± 13.3) nM. This binding is not Src kinase activity-dependent and the dysfunctions of the SH2 and/or SH3 domains do not significantly affect the binding. Thus, we have provided direct experimental evidence indicating that the SH2 and SH3 domains may function to promote catalytic activity of active n-Src, which is important in the regulation of NMDAR functions.

Introduction

Src family kinases (SFKs) are critically involved in the regulation of many biological functions mediated through growth factors, G-protein-coupled receptors, or ligand-gated ion channels. As such, SFKs have become important targets for therapeutic treatments [1;2]. Based on the crystallographic studies of inactive and active Src, the SH2 and SH3 domains are believed to form a ‘regulatory apparatus’. The binding of the phosphorylated C-tail to the SH2 domain and/or the binding of the SH2-kinase linker to the SH3 domain inactivates SFKs [3–6]. It has been shown that either mutating tyrosine 527 to phenylalanine (Y527F) in the C-tail of chicken c-Src, dephosphorylating phosphorylated Y527, or breaking the SH2 or SH3 domain interactions by dysfunction of either of these domains may significantly enhance the enzyme activity of c-Src [3–6].

It is known that NMDARs are regulated by receptor-associated SFKs [7–12]. This regulation is found to be a key mechanism underlying the activity-dependent neuroplasticity associated with many physiological and pathological processes [11–13]. The C-termini of

Address correspondence to: Xian-Min Yu, 1115 West Call Street, Tallahassee, FL 32306-4300. Tel: 850-645-2718; Fax: 850-644-5781; xianmin.yu@med.fsu.edu.

NMDA NR2A and NR2B subunits are primary targets for phosphorylation by SFKs, such as Src and Fyn [14–16]. However, the mechanism by which NMDARs are regulated by SFKs is still not completely understood.

To elucidate how NMDARs are regulated by Src kinase, we examined the regulation of NMDA NR1-1a/NR2A receptors, which represent a dominant NMDAR subunit combination in the adult central nervous system (CNS), by Src both in cell culture and *in-vitro*. Our results revealed that the SH2 and SH3 domain interactions may act not only to constrain the activation of Src, but also to promote the enzyme activity of activated Src, which is important in the regulation of NMDARs by Src.

Results and Discussion

NMDA NR1-1a/NR2A receptors were co-expressed in HEK-293 cells expressing viral Src (v-Src), wild-type neuronal Src (n-Src) or n-Src mutants. Whole-cell currents were evoked with L-aspartate or NMDA (250 μM) applied through a double-barrel pipette system. Figure 1A shows a recording of NMDAR-mediated current traces before and after the application of the SFK inhibitor, PP2 (10 μM). Co-transfection of constitutively active Src, such as v-Src, significantly enhanced NMDA NR1-1a/NR2A receptor-mediated current density when compared with that recorded in cells without v-Src expression (Fig. 1C). The averaged peak amplitude of whole-cell currents recorded in HEK-293 cells expressing constitutively active n-Src, in which tyrosine 535 (corresponding to Y527 in chicken c-Src) was mutated to phenylalanine (Y535F) (see Table 1), was 760 ± 140 pA (n = 12, mean ± SEM). Application of the SFK inhibitor, PP2, significantly inhibited NR1-1a/NR2A receptor-mediated whole-cell currents (Fig. 1A) without altering reversal potential of recorded currents (Fig. 1B). The peak amplitudes of NMDA currents were reduced to 73 ± 7% (n = 7) of that prior to PP2 application (Fig. 1D). In contrast, application of PP3, the inactive form of PP2, produced no such effect (Fig. 1D). Consistent with results reported previously [7;17], no significant change in NMDAR currents could be induced by PP2 application in cells without Src co-transfection (Fig. 1D). No significant effect of PP2 was detected on NMDAR currents in cells co-expressing n-Src (K303R/Y535F) in which lysine at residue 303 in the kinase domain was mutated to arginine (Table 1), thereby blocking the enzyme activity of Src [3;18]. Peak amplitudes of NMDAR currents during PP2 application were 96 ± 4% (n = 7) of controls before PP2 application (Fig. 1D). Taken together, these data demonstrate that through inhibiting the activity of Src expressed in recorded cells, PP2 application depresses NR1-1a/NR2A receptor activity.

Unexpectedly, however, the inhibition of NMDAR currents induced by PP2 application was significantly reduced in cells expressing n-Src/Y535F with additional mutations of D101N and R183K in the SH3 and SH2 domains (Fig. 1D, Table 1). Previous studies [3;18–21] have demonstrated that D99 (corresponding to D101 in n-Src) in the SH3 domain of c-Src forms a salt bridge with an arginine three residues upstream of the conserved PXXP motif of the SH3 ligand. The D99N mutation prevents the formation of this salt bridge and disrupts the SH3 binding specificity. R175 (corresponding to R183 in n-Src) in the SH2 domain of c-Src makes important connections with phosphorylated tyrosine. Mutation of R175 to lysine prevents this connection and decreases SH2 interactions with its ligand. D99N and R175K mutations therefore inhibit the interactions with ligands of the SH3 and SH2 domains, respectively, both intra- and inter-molecularly and thereby disrupt the overall functions of Src kinase [3;18–21].

Following PP2 application, peak amplitudes of NMDAR currents were reduced to 89 ± 3% (n = 7) of controls before PP2 application in cells co-expressing active n-Src with dysfunctional SH3 and SH2 domains (D101N/R183K/Y535F, Fig. 1D). This inhibition of

NMDAR currents was significantly ($p < 0.05$, independent group t-test) smaller than that detected in cells co-expressing constitutively active n-Src (Y535F, Fig. 1D), raising a question: What roles do the SH3 and/or SH2 domains play in the regulation of NMDARs by active Src?

To address this issue we examined the activity of n-Src expressed in HEK-293 cells. The gel shown in Fig. 2A was loaded with the lysates of HEK-293 cells expressing wild-type n-Src and its mutants, respectively. Consistent with previous findings [3;17], the mutation of Y535F significantly increased phosphorylation at Y424 (corresponding to Y416 in chicken c-Src) when compared with that in wild-type n-Src (Fig. 2A). The dysfunction of the kinase domain abolished the phosphorylation of Y424 of constitutively active n-Src (K303R/Y535F, Fig. 2A). However, it was also noted that the phosphorylation of the activation loop, represented by the phosphorylation of Y424, in n-Src mutants with defective SH2 and/or SH3 domains was reduced when compared with that in constitutively active n-Src (Y535F, Fig. 2A). These findings suggest that the dysfunction of the SH3 (D101N) and/or SH2 (R183K) domains may down-regulate the activity of active Src.

We then examined the enzyme activity in lysates of HEK-293 cells expressing n-Src or its mutants by measuring the phosphorylation of the generic substrate, poly-Glu-Tyr (Sigma). We found that the kinase activity in cells expressing constitutively active n-Src was significantly increased over that of cells expressing wild-type n-Src (WT, Fig. 2B). The expression of inactive n-Src (K303R/Y535F) did not produce detectable kinase activity (Fig. 2B). Compared to cells expressing constitutively active n-Src, the kinase activity was significantly reduced by 27 ± 4% in cells expressing active n-Src with a dysfunctional SH3 domain (D101N/Y535F), by 96 ± 0.05% in cells expressing active n-Src with a dysfunctional SH2 domain (R183K/Y535F), and by 97 ± 0.04% in cells expressing active n-Src with dysfunctional SH3 and SH2 domains (D101N/R183K/Y535F, Fig. 2B). These data not only suggest that the dysfunction of the SH3 and/or SH2 domains significantly reduces the enzyme activity of active Src expressed in HEK-293 cells, but also show that the SH2 domain plays a larger role than does the SH3 domain in the regulation of n-Src activity. Consistent with the finding that the dysfunction of the SH3 and SH2 domains dramatically reduced n-Src activity (Fig. 2B), we also found that when compared with constitutively active n-Src (Y535F), neither autophosphorylation in the activation loop nor kinase activity could be detected in the n-Src mutant, $Y535F^{\Delta 1–258}$, in which the N-terminus and both the SH3 and SH2 domains were deleted (Supplemental Fig. 1).

To confirm the effect produced by the SH3 and/or SH2 domain dysfunctions, n-Src and its mutants were expressed in BL21(DE3) cells and purified as described previously [22] and examined. Figure 3A shows these purified proteins. Kinase activity on the generic substrate, poly-Glu-Tyr, was measured at 5 to 60 min after the addition of n-Src or its mutants (0.5 μM, Fig. 3B). Consistent with our previous findings [22], the enzyme activity of constitutively active n-Src protein was significantly enhanced when compared to wild-type n-Src (Fig. 3B) while no enzyme activity was detected in inactive n-Src protein (Fig. 3B). Mutation of the SH3 or SH2 domain significantly inhibited Src kinase activity with a greater effect produced by dysfunction of the SH2 domain (Fig. 3B) as was noted in HEK-293 cells.

Furthermore, we examined the autophosphorylation of constitutively active n-Src, active n-Src with dysfunctional SH3 and SH2 domains and inactive n-Src. Five μg of each of these proteins were respectively treated with a buffer containing Lambda Protein Phosphatase (λPPase, 400 U) (New England BioLabs) for 18 hrs at 30°C. To initiate autophosphorylation, a buffer containing 10 mM sodium orthovanadate, 50 mM sodium fluoride, 0.2 mM ATP and 10 mM $MgCl_2$ was added into the samples to inactivate the phosphatase for 0, 5, 10, or 20 min. The phosphorylation reaction was then stopped by the

addition of 6× SDS sample buffer supplemented with 50 mM EDTA. Y424 phosphorylation was subsequently analyzed by Western blot (Fig. 3C). Ratios of band intensity detected with anti-Src^{pY416} antibody (rabbit) versus that detected with anti-Src antibody (mouse) were calculated and normalized to the ratio detected in n-Src/Y535F protein that was not treated with λPPase (Fig. 3C). A decreased phosphorylation at Y424 was observed in the active n-Src with dysfunctional SH3 and/or SH2 domains when compared with that in the constitutively active n-Src (Fig. 3C). However, 5 min after inactivation of λPPase Y424 phosphorylation of the active n-Src without and with dysfunctional SH3, SH2 and both SH3 and SH2 domains reached similar levels (75.4 ± 0.8%, 61.4 ± 9.8%, 75.0 ± 8.4% and 79.3 ± 3.4%) of their respective phosphorylation at 20 min. No such phosphorylation was observed in inactive n-Src (Fig. 3C). Collectively, these data suggest that the dysfunction of the SH3 or SH2 domains does not alter the ability of active Src to phosphorylate itself at Y424, but significantly reduces autophosphorylation through modulating kinase activity of the enzyme.

To determine the roles of the SH3 and/or SH2 domains in the Src regulation of NMDAR phosphorylation, the protein fragment corresponding to amino acids K1096-V1464 in NR2A C-tail was incubated with wild-type n-Src or its mutants at a 1:1 concentration ratio for 1 hr at 37 °C in the presence of 10 mM $MgCl_2$ and 0.2 mM ATP. We found that the NR2A C-tail protein was phosphorylated by wild-type n-Src, but not by the inactive n-Src (Fig. 4A). Incubation with the active n-Src produced an increased level of NR2A C-tail phosphorylation over that incubated with wild-type n-Src. Active n-Src proteins with defective SH3 and/or SH2 domains produced a reduced level of NR2A C-tail phosphorylation when compared to the constitutively active Src (Fig. 4A). The phosphorylation time course of the NR2A C-tail protein by wild-type and mutant n-Src proteins is shown in Fig. 4B. Consistently, the highest tyrosine phosphorylation was produced by the constitutively active n-Src. At 10 min, the phosphorylation of NR2A C-tail by the constitutively active n-Src had reached a level similar to that produced by the wild-type n-Src at 60 min (Fig. 4B). Remarkably, dysfunction of the SH3 and/or SH2 domains impacted the phosphorylation process of NR2A C-tail proteins by active n-Src and reduced the n-Src activity on NMDARs, with the larger effect produced by the dysfunction of the SH2 domain (Fig. 4).

To determine if the reduced phosphorylation and activity of NMDARs observed with dysfunction of the SH3 and/or SH2 domains in Src may be due to a change in the interaction of Src with its substrate, the binding of wild-type or mutant n-Src proteins with the NR2A C-tail protein was examined using Surface Plasmon Resonance (SPR, Fig. 5). We found that, in contrast to bovine serum albumin (BSA), all of the n-Src proteins were able to bind NR2A C-tail with similar, nanomolar-range binding affinities (Fig. 5). This indicates that the ability of n-Src protein to bind to the NR2A C-tail is independent of its kinase activity, and that dysfunction of the SH3 and/or SH2 domains does not affect this interaction.

The regulation of NMDARs by Src and other SFKs [7–12] has been found to be a key mechanism underlying the activity-dependent neuroplasticity in the CNS. Through binding to PSD-95 [23] or ND2 [24], SFKs are closely linked to NMDARs in neurons [12]. It is well known that the activity of SFKs is tightly regulated by the reversible phosphorylation of Y527 in chicken c-Src *in-vivo*. The phosphorylation of Y527 may decrease the activity of SFKs, with dephosphorylation of phosphorylated Y527 eliciting the opposite effect [3–6]. Protein tyrosine phosphatase alpha (PTPα) may selectively dephosphorylate phosphorylated Y527 [25;26] while C-terminal Src kinase (Csk) specifically phosphorylates Y527 [3;27;28]. PTPα associates with NMDARs through binding to the scaffold protein, PSD-95, and constitutively up-regulates NMDARs through endogenous SFKs [29]. Csk binds to phosphorylated NMDARs in response to the actions of SFKs, depresses SFKs and thereby down-regulates NMDARs [17]. The close proximity of Csk, PTPα, SFKs and their substrate,

NMDARs, ensures that the complex forms a well-controlled molecular network regulating receptor function and synaptic plasticity [9;11;12;17;29].

Two types of Src, cellular (c-Src) and neuronal Src (n-Src), can be found in neurons. n-Src contains a six-amino acid insertion in the SH3 domain and is only expressed in neurons [3]. The SH3 and SH2 domains in Src have been recognized to be involved in the negative regulation of Src. However, it has also been shown that the SH2 domain may exert positive effects on the kinase activity and substrate interaction with the kinase domain, for example, in v-Fps tyrosine kinase [30;31]. Recent detailed investigations demonstrated that in active Fps kinase, the SH2 domain tightly interacts with the kinase N-terminal lobe and positions the kinase αC helix in an active configuration. This structure is stabilized by ligand binding to the SH2 domain [32]. Similarly, in active c-Abl tyrosine kinase, the SH2 and SH3 domains redistribute from their autoinhibitory positions on the backside of the kinase domain to adopt an extended conformation, stimulating the catalytic activity of the kinase [32]. Small-angle X-ray scattering (SAXS) analysis shows that in activated c-Abl there is an extended array of the SH3, SH2, and kinase domains. This alternative conformation may prolong the active state of the kinase by preventing it from returning to the autoinhibitory state [33]. In Src and Abl kinases, the SH2 domain can act in conjunction with an additional SH2 or SH3 domain to maintain an inactive state through intramolecular interactions with the catalytic domain, but is also critical for active signaling [32]. Therefore, it is possible that the SH2 domain is bifunctional in the regulation of kinase activity.

A previous study [14] reported that the tyrosine phosphorylation of NMDA NR2A and NR2B subunits induced by incubation with recombinant Src and Fyn may be significantly reduced by application of SH2 domain binding peptides. This could be induced by blocking the binding of the SH2 domain to the substrate and thereby preventing the interaction of the substrate with the kinase domain. We found that with active n-Src in which the C-tail tyrosine was mutated to phenylalanine, dysfunctions of SH2 and/or SH3 domains reduced the autophosphorylation of the kinase domain activation loop, depressed kinase activity, and inhibited Src-mediated NMDAR tyrosine phosphorylation and channel activity regulation. Although detailed mechanisms underlying the actions of SH2 and SH3 domains in the regulation of active n-Src remain to be clarified, our study has revealed that the SH2 and SH3 domain interactions may act not only to constrain the activation of n-Src, but also to regulate the enzyme activity of active n-Src, in which the SH2 domain appears to play a greater role than the SH3 domain. These findings may be very important for understanding the regulation of activity-dependent neuroplasticity in the CNS.

Experimental Procedures

HEK-293 cell culture and transfection

Cell culture and DNA transfection were performed as described previously [17;29]. Briefly, HEK-293 cells were grown in Dulbecco's Modified Eagles Media (DMEM) (Invitrogen, Carlsbad, CA, USA) supplemented with 10% fetal bovine serum (FBS) (Invitrogen). These cells were then transfected using the Effecten (Qiagen, Valencia, CA, USA) or Lipofectamine (Gibco-BRL, Carlsbad, CA, USA) method as per the manufacturer's instructions with expression vectors (pcDNA3 or pRcCMV) containing cDNAs encoding NR1-1a (0.4 μg), NR2A (1.2 μg) and/or v-Src (0.2 μg), wild-type n-Src (0.2 μg) or one type of n-Src mutant (0.2 μg): Y535F, D101N/Y535F, R183K/Y535F, K303R/Y535F, D101N/R183K/Y535F, $Y535F^{\Delta 1-258}$ or $K303R/Y535F^{\Delta 1-258}$. D101, R183, K303 or Y535 in mouse n-Src correspond to D99, R175, K297, and Y527 in chicken c-Src, respectively (see Table 1). For electrophysiological recordings, green fluorescence protein (GFP, 0.15 μg) was co-transfected. After 5–12 hrs, transfected cells were maintained in the DMEM supplemented with AP5 (500 μM) for 48 hrs before experiments.

Whole-cell recordings in cultured cells

Methods for whole-cell patch clamp recordings in HEK-293 cells have been described in our previous works [17;29]. In brief, cells were bathed in a standard extracellular solution containing NaCl (140), CsCl (5), $CaCl_2$ (1.2), HEPES (25), glucose (32), TTX (0.001), glycine (0.01), pH: 7.35 and osmolarity: 310–320 mOsm. Recording pipettes were pulled to a diameter of 1 – 2 μm at the tip and filled with intracellular solution composed of (in mM): CsCl (145), BAPTA (0.5), HEPES (10), $MgCl_2$ (2), K-ATP (4), osmolarity 290–300 mOsm (DC resistance: 4–7 MΩ). Whole-cell currents were evoked by application of L-aspartate or NMDA (250 μM) dissolved in the extracellular solution for 3 sec via a multi-barrel fast-step perfusion system (SF-77B perfusion fast-step system, Warner Instrument, Hamden, CT, USA). Recordings were conducted under the voltage-clamp condition at a holding potential of −60 mV. Whole-cell currents were recorded using Axopatch 200B amplifiers (Molecular Devices, Sunnydale, CA, USA). On-line data acquisition and off-line analysis were performed using pClamp9 software (Molecular Devices).

Protein expression and purification

Techniques used for protein expression and purification were described previously [22]. In brief, cDNA encoding full length wild-type n-Src, n-Src mutants (Y535F, D101N/Y535F, R183K/Y535F, K303R/Y535F or D101N/R183K/Y535F) or aa K1096-V1464 of the NR2A subunit was cloned into the pET15b vector and subsequently transformed into *E. coli* BL21(DE3) cells. The proteins were expressed as N-terminal His_6 tag fusions in Terrific Broth supplemented with 100 μg/mL of ampicillin using the modified Autoinduction™ protocol [34]. Cultures were grown at 37°C for 3–4 hrs and then cooled to 18°C for protein expression for additional 18 hrs. Cells were then harvested by centrifugation at 7,500 g for 15 mins at 4°C. Pellets were resuspended in buffer A (50 mM Tris-Cl, 0.5 M NaCl, 25 mM imidazole, pH 8.0) containing 1 mM phenylmethylsulphonyl fluoride (PMSF) and lysed using a sonicator. After centrifugation at 25,000 g at 4°C, the supernatant was loaded on a Chelating Sepharose column (Amersham Biosciences, Uppsala, Sweden). After the initial wash with Buffer A, proteins were eluted with 500 mM imidazole. The His tag was removed by incubation with thrombin for 4 hrs at 37°C. Protein purity was assessed using SDS-PAGE and Western blotting (Fig. 2B) and was shown to be at least 95%. Purified proteins were concentrated following extensive dialysis in buffer containing 30 mM sodium phosphate and 30 mM NaCl (pH 7.4), and stored at 4°C under reducing conditions (1 mM DTT), and then analyzed with electrospray ionization (ESI) linear ion trap mass spectrometer (LTQ MS) (Thermo Finnigan, Waltham, MA, USA). The sequence coverage of purified n-Src proteins was determined after analysis of respective tryptic peptides using MS/MS [22]. Protein concentration was determined spectrophotometrically in the presence of 6 M urea at 280 nm using calculated extinction coefficients (www.expasy.org).

Immunoblotting and in-vitro kinase activity assay

Proteins purified from BL21(DE3) cells were subjected to SDS-PAGE and Western blotting. Antibodies including anti-Src antibody (Millipore, Billerica, MA, USA), anti-pY527 antibody (Cell Signaling, Danvers, MA, USA), anti-pY416 antibody (Cell Signaling), anti-NR2A C-tail antibody (Upstate, Charlottesville, VA, USA) and anti-phosphotyrosine antibody (4G10, Upstate) were used. To determine the kinase activity of the n-Src proteins, a modified ELISA-based assay (PTK101, Sigma, St. Louis, MO, USA) was performed using an exogenous tyrosine kinase-specific polymer substrate, poly-Glu-Tyr, or an NR2A protein fragment corresponding to the C-tail amino acids K1096-V1464. The phosphorylation reaction was initiated by the addition of n-Src proteins to the tyrosine kinase reaction buffer containing excess Mg^{2+} (10 mM), Mn^{2+} (10 mM) and ATP (0.2 mM) in microtiter plates coated with poly-Glu-Tyr substrate or NR2A C-tail. The phosphorylation reactions were stopped by removing the reaction mixture and washing with phosphate buffered saline

Tween-20 (PBST) at each time point as indicated. The phosphorylated substrate was detected with a horseradish peroxidase (HRP)-conjugated anti-phosphotyrosine antibody. A color reaction was induced by adding HRP substrate *o*-Phenylenediamine (OPD) and stopped with 0.25 M sulfuric acid, followed by absorbance measurement at 490 nm with a spectrophotometer in a microplate ELISA reader (Benchmark, BioRad, Hercules, CA, USA). Steady-state kinase activity assays for the proteins were carried out at room temperature for 60 min. All of the chemicals and agents were purchased from Sigma except where indicated.

To examine the autophosphorylation of the proteins, 5 μg of n-Src/Y535F, n-Src/D101N/Y535F, n-Src/R183K/Y535F, n-Src/D101N/R183K/Y535F, or n-Src/K303R/Y535F were dephosphorylated with 400U of Lambda Protein Phosphatase (New England BioLabs, Ipswich, MA, USA) in the manufacturer-provided reaction buffer at 30°C for 18 hrs. The phosphatase was inactivated by the addition of 10 mM sodium orthovanadate and 50 mM sodium fluoride included in a buffer containing 0.2 mM ATP and 10 mM $MgCl_2$ for 0, 5 10 or 20 min. The reactions were stopped by the addition of 6× SDS sample buffer supplemented with 50 mM EDTA. Autophosphorylation at pY424 was analyzed by Western blot and quantified by densitometric analysis using Image J (NIH, Bethesda, MD, USA).

Surface Plasmon Resonance

The affinity interactions of Src mutants and NR2A C-tail fragment were analyzed using a Biacore T-100 optical biosensor (Biacore/GE Healthcare, Uppsala, Sweden). NR2A C-tail protein fragment was immobilized on a CM5 chip using amine coupling chemistry. This process consisted of surface chip activation with a 1:1 ratio of EDS/NHS (0.4 M 1-ethyl-3-(3-dimethylaminopropyl)-carboimide and 0.1M N-hydroxysuccinimide), followed by NR2A C-tail protein immobilization to 2000 RU using 10 μg/mL protein in 10 mM sodium acetate immobilization buffer (pH 4.5), and chip surface deactivation with 1M ethanolamine-HCl (pH 8.5). All binding experiments were carried out in a running buffer containing 50 mM HEPES, 150 mM NaCl, 3 mM EDTA, 0.05% p20, pH 7.4. Src concentrations of up to 400 μM were injected in triplicate over the chip surface at a flow rate of 10 μL/min for 180 sec. The surface was regenerated with 30 sec bursts of 2 M NaCl followed by 0.05% SDS at a flow rate of 50 μL/min. All experiments were repeated over a second CM5 chip in triplicate following the same protocol. The data were analyzed using BiaEvaluation 3.0 software (Biacore) and SigmaPlot (Systat Software Inc, Richmond, CA, USA) and fit to a 1:1 Langmuir binding model for calculation of the equilibrium dissociation constants (K_D).

Supplementary Material

Refer to Web version on PubMed Central for supplementary material.

Acknowledgments

This work was supported by a grant from NIH (R01 NS053567) to X.-M.Y. Plasmids of v-Src, and n-Src and its mutants were kindly provided by Drs. T. Pawson (University of Toronto) and S. Hanks (Vanderbilt University [18]), respectively. We gratefully acknowledge the Biomedical Proteomics Laboratory at the College of Medicine, FSU, for the use of UV/Vis spectroscopy and surface plasmon resonance instrumentation.

Reference List

1. Cohen P. Protein kinases--the major drug targets of the twenty-first century? Nat Rev Drug Discov. 2002; 1:309–315. [PubMed: 12120282]
2. Liu XJ, Gingrich JR, Vargas-Caballero M, Dong YN, Sengar A, Beggs S, Wang SH, Ding HK, Frankland PW, Salter MW. Treatment of inflammatory and neuropathic pain by uncoupling Src from the NMDA receptor complex. Nat Med. 2008; 14:1325–1332. [PubMed: 19011637]

3. Brown MT, Cooper JA. Regulation, substrates and functions of src. Biochim Biophys Acta. 1996; 1287:121–149. [PubMed: 8672527]
4. Xu W, Harrison SC, Eck MJ. Three-dimensional structure of the tyrosine kinase c-Src. Nature. 1997; 385:595–602. [PubMed: 9024657]
5. Ingley E. Src family kinases: regulation of their activities, levels and identification of new pathways. Biochim Biophys Acta. 2008; 1784:56–65. [PubMed: 17905674]
6. Roskoski R Jr. Src kinase regulation by phosphorylation and dephosphorylation. Biochem Biophys Res Commun. 2005; 331:1–14. [PubMed: 15845350]
7. Kohr G, Seeburg PH. Subtype-specific regulation of recombinant NMDA receptor-channels by protein tyrosine kinases of the src family. J Physiol (Lond). 1996; 492 (Pt 2):445–452. [PubMed: 9019541]
8. Miyakawa T, Yagi T, Kitazawa H, Yasuda M, Kawai N, Tsuboi K, Niki H. Fyn-kinase as a determinant of ethanol sensitivity: relation to NMDA-receptor function. Science. 1997; 278:698–701. [PubMed: 9381182]
9. Yu XM, Askalan R, Keil GJI, Salter MW. NMDA channel regulation by channel-associated protein tyrosine kinase Src. Science. 1997; 275:674–678. [PubMed: 9005855]
10. Hisatsune C, Umemori H, Mishina M, Yamamoto T. Phosphorylation-dependent interaction of the N-methyl-D-aspartate receptor epsilon 2 subunit with phosphatidylinositol 3-kinase. Genes Cells. 1999; 4:657–666. [PubMed: 10620012]
11. Ali DW, Salter MW. NMDA receptor regulation by Src kinase signalling in excitatory synaptic transmission and plasticity. Curr Opin Neurobiol. 2001; 11:336–342. [PubMed: 11399432]
12. Salter MW, Kalia LV. Src kinases: a hub for NMDA receptor regulation. Nat Rev Neurosci. 2004; 5:317–328. [PubMed: 15034556]
13. MacDonald JF, Jackson MF, Beazely MA. Hippocampal long-term synaptic plasticity and signal amplification of NMDA receptors. Crit Rev Neurobiol. 2006; 18:71–84. [PubMed: 17725510]
14. Cheung HH, Gurd JW. Tyrosine phosphorylation of the N-methyl-D-aspartate receptor by exogenous and postsynaptic density-associated Src-family kinases. J Neurochem. 2001; 78:524–534. [PubMed: 11483655]
15. Nakazawa T, Komai S, Tezuka T, Hisatsune C, Umemori H, Semba K, Mishina M, Manabe T, Yamamoto T. Characterization of Fyn-mediated Tyrosine Phosphorylation Sites on GluRepsilon 2 (NR2B) Subunit of the N-Methyl-D-aspartate Receptor. J Biol Chem. 2001; 276:693–699. [PubMed: 11024032]
16. Yang M, Leonard JP. Identification of mouse NMDA receptor subunit NR2A C-terminal tyrosine sites phosphorylated by coexpression with v-Src. J Neurochem. 2001; 77:580–588. [PubMed: 11299320]
17. Xu J, Weerapura M, Ali MK, Jackson MF, Li H, Lei G, Xue S, Kwan CL, Manolson MF, Yang K, MacDonald JF, Yu XM. Control of excitatory synaptic transmission by C-terminal Src kinase. J Biol Chem. 2008; 283:17503–17514. [PubMed: 18445593]
18. Polte TR, Hanks SK. Complexes of focal adhesion kinase (FAK) and Crk-associated substrate (p130(Cas)) are elevated in cytoskeleton-associated fractions following adhesion and Src transformation. Requirements for Src kinase activity and FAK proline-rich motifs. J Biol Chem. 1997; 272:5501–5509. [PubMed: 9038154]
19. Weng Z, Rickles RJ, Feng S, Richard S, Shaw AS, Schreiber SL, Brugge JS. Structure-function analysis of SH3 domains: SH3 binding specificity altered by single amino acid substitutions. Mol Cell Biol. 1995; 15:5627–5634. [PubMed: 7565714]
20. Songyang Z, Cantley LC. Rocognition and specificity in protein tyrosine kinase-mediated signalling. TIBS. 1995; 20:470–475. [PubMed: 8578591]
21. Verderame MF. pp60v-src transformation of rat cells but not chicken cells strongly correlates with low-affinity phosphopeptide binding by the SH2 domain. Mol Biol Cell. 1997; 8:843–854. [PubMed: 9168470]
22. Marin V, Groveman BR, Qiao H, Xu J, Ali MK, Fang XQ, Lin SX, Rizkallah R, Hurt MH, Bienkiewicz EA, Yu XM. Characterization of neuronal Src kinase purified from a bacterial expression system. Protein Expr Purif. 2010; 74:289–297. [PubMed: 20558296]

23. Tezuka T, Umemori H, Akiyama T, Nakanishi S, Yamamoto T. PSD-95 promotes Fyn-mediated tyrosine phosphorylation of the N-methyl-D-aspartate receptor subunit NR2A. Proc Natl Acad Sci USA. 1999; 96:435–440. [PubMed: 9892651]
24. Gingrich JR, Pelkey KA, Fam SR, Huang Y, Petralia RS, Wenthold RJ, Salter MW. Unique domain anchoring of Src to synaptic NMDA receptors via the mitochondrial protein NADH dehydrogenase subunit 2. Proc Natl Acad Sci U S A. 2004; 101:6237–6242. [PubMed: 15069201]
25. Ponniah S, Wang DZ, Lim KL, Pallen CJ. Targeted disruption of the tyrosine phosphatase PTPalpha leads to constitutive downregulation of the kinases Src and Fyn. Curr Biol. 1999; 9:535–538. [PubMed: 10339428]
26. Su J, Muranjan M, Sap J. Receptor protein tyrosine phosphatase alpha activates Src-family kinases and controls integrin-mediated responses in fibroblasts. Curr Biol. 1999; 9:505–511. [PubMed: 10339427]
27. Nada S, Okada M, MacAuley A, Cooper JA, Nakagawa H. Cloning of a complementary DNA for a protein-tyrosine kinase that specifically phosphorylates a negative regulatory site of p60c-src. Nature. 1991; 351:69–72. [PubMed: 1709258]
28. Imamoto A, Soriano P. Disruption of the csk gene, encoding a negative regulator of Src family tyrosine kinases, leads to neural tube defects and embryonic lethality in mice. Cell. 1993; 73:1117–1124. [PubMed: 7685657]
29. Lei G, Xue S, Chery N, Liu Q, Xu J, Kwan CL, Fu Y, Lu YM, Liu M, Harder KH, Yu XM. Gain control of N-methyl-D-aspartate receptor activity by receptor-like protein tyrosine phopshatase alpha. The EMBO J. 2002; 21:2977–2989.
30. Stone JC, Atkinson T, Smith M, Pawson T. Identification of functional regions in the transforming protein of Fujinami sarcoma virus by in-phase insertion mutagenesis. Cell. 1984; 37:549–558. [PubMed: 6327075]
31. Sadowski I, Stone JC, Pawson T. A noncatalytic domain conserved among cytoplasmic protein-tyrosine kinases modifies the kinase function and transforming activity of Fujinami sarcoma virus P130gag-fps. Mol Cell Biol. 1986; 6:4396–4408. [PubMed: 3025655]
32. Filippakopoulos P, Kofler M, Hantschel O, Gish GD, Grebien F, Salah E, Neudecker P, Kay LE, Turk BE, Superti-Furga G, Pawson T, Knapp S. Structural coupling of SH2-kinase domains links Fes and Abl substrate recognition and kinase activation. Cell. 2008; 134:793–803. [PubMed: 18775312]
33. Nagar B, Hantschel O, Seeliger M, Davies JM, Weis WI, Superti-Furga G, Kuriyan J. Organization of the SH3-SH2 unit in active and inactive forms of the c-Abl tyrosine kinase. Mol Cell. 2006; 21:787–798. [PubMed: 16543148]
34. Grabski A, Mehler M, Drott D. The Overnight Express Autoinduction System: High-density cell growth and protein expression while you sleep. Nat Meth. 2005; 2:233–235.

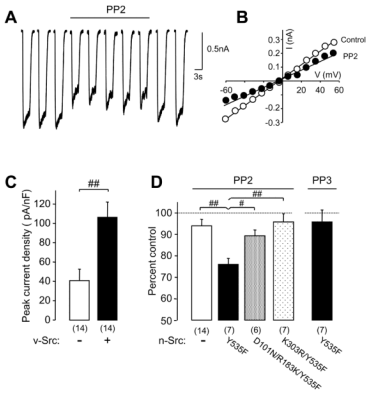

Figure 1. Effects of inactivation of the SH3 and SH2 domains on the Src regulation of NMDAR activity

A: An example showing NR1-1a/NR2A receptor-mediated whole-cell currents before and during PP2 application recorded from HEK-293 cells co-transfected with cDNAs of n-Src/Y535F; B: An example of the current-voltage relationship recorded before (control) and during PP2 application from a cells co-transfected with n-Src/Y535F; C: Summary data (mean ± SEM) showing NMDAR peak current density recorded in HEK-293 cells transfected without ("−") or with ("+") v-Src. D: Summary data showing effects of PP2 application on peak amplitudes of NMDAR currents, which were normalized with those before PP2 application (= 100%, dashed line), recorded from cells co-transfected without ("−") or with cDNAs of n-Src mutants as indicated; #: $p<0.05$, ##: $p<0.01$ (Independent group t-test). Values in brackets indicate the number of cells tested.

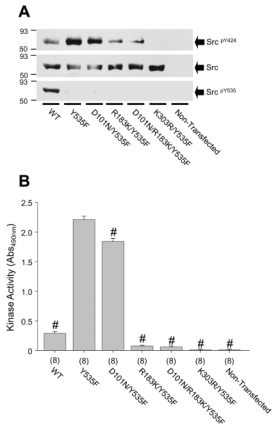

Figure 2. Effects of dysfunction of the SH3 and/or SH2 domains on n-Src proteins expressed in HEK-293 cells

A: Western blot showing protein expression in lysates (20 μg) of HEK-293 cells. The filters were sequentially immunoblotted with antibodies towards the proteins as indicated next to arrows. Src^{pY535} (corresponding to Src^{pY527}): probed with anti-pY527 antibody (Rabbit); Src^{pY424} (corresponding to Src^{pY416}): probed with anti-pY416 antibody (Rabbit). Src: probed with anti-Src antibody (Mouse). Values left of the blots indicate molecular mass in kilodaltons. B: Summary data showing kinase activity of n-Src proteins expressed in HEK-293 cells on a generic substrate (poly-Glu-Tyr); Values in brackets indicate number of experimental repeats. #: $p<0.05$ (Independent group t-test) in comparison with the kinase activity of constitutively active n-Src (Y535F).

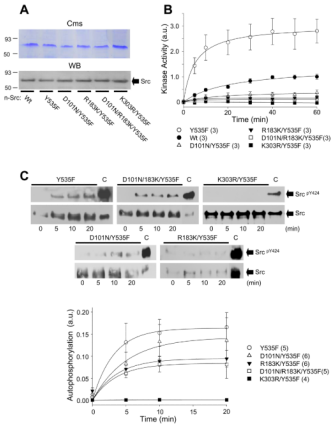

Figure 3. Effects of dysfunction of the SH3 and/or SH2 domains on purified n-Src proteins *in-vitro*

A: Purified n-Src proteins expressed in BL21(DE3) cells. Cms: Coomassie blue staining. WB: Western blot of purified n-Src proteins probed with anti-Src antibody. B: Summary data showing kinase activity on a generic substrate (poly-Glu-Tyr) for purified n-Src proteins as indicated. C: Western blot showing n-Src autophosphorylation of Y424. The filters were sequentially immunoblotted with antibodies towards the proteins as indicated next to arrows. C: Untreated n-Src/Y535F protein. The graph shows summary data from densitometric analysis of Western blot data displayed as a ratio of pY424 to total Src normalized to untreated constitutively active n-Src (Y535F); Values in brackets indicate the number of experimental repeats.

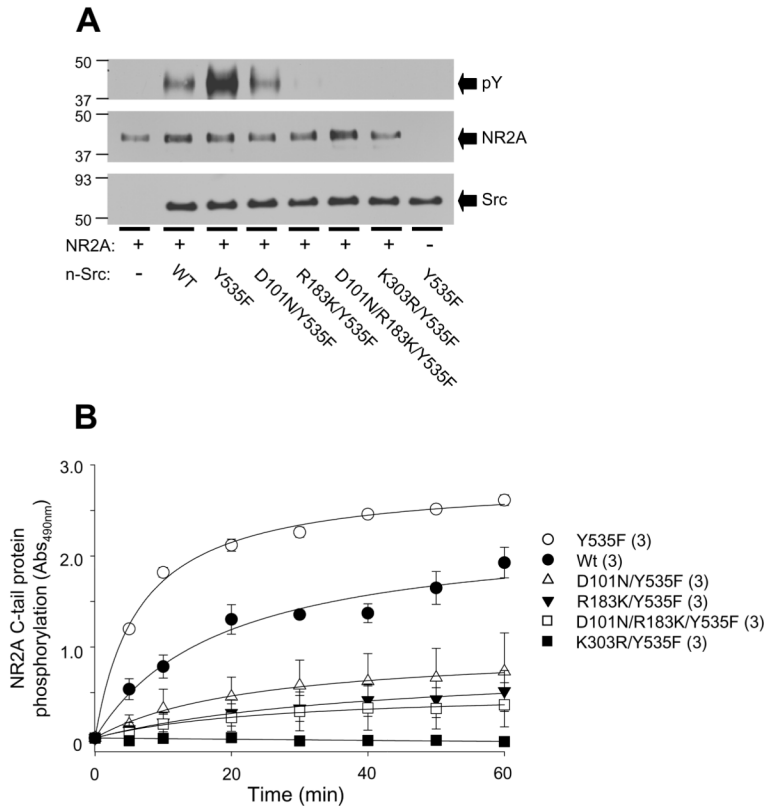

Figure 4. Effects of dysfunction of the SH3 and/or SH2 domains on the phosphorylation of NMDA NR2A C-tail protein by n-Src

A: Western blot showing phosphorylation of NR2A C-tail fragment proteins (aa 1096–1464, 5 μg) incubated without ("−") or with ("+") n-Src or its mutants as indicated. Duplicate filters were immunoblotted with antibodies towards the proteins as indicated next to arrows. NR2A: probed with anti-NR2A C-tail antibody (Rabbit); pY: probed with anti-phosphotyrosine antibody (4G10, Mouse); Src: probed with anti-Src antibody (Mouse). B: Summary data showing NR2A C-tail phosphorylation induced by n-Src proteins as indicated and detected by color assay (see Experimental Procedure). Values in brackets indicate number of experimental repeats.

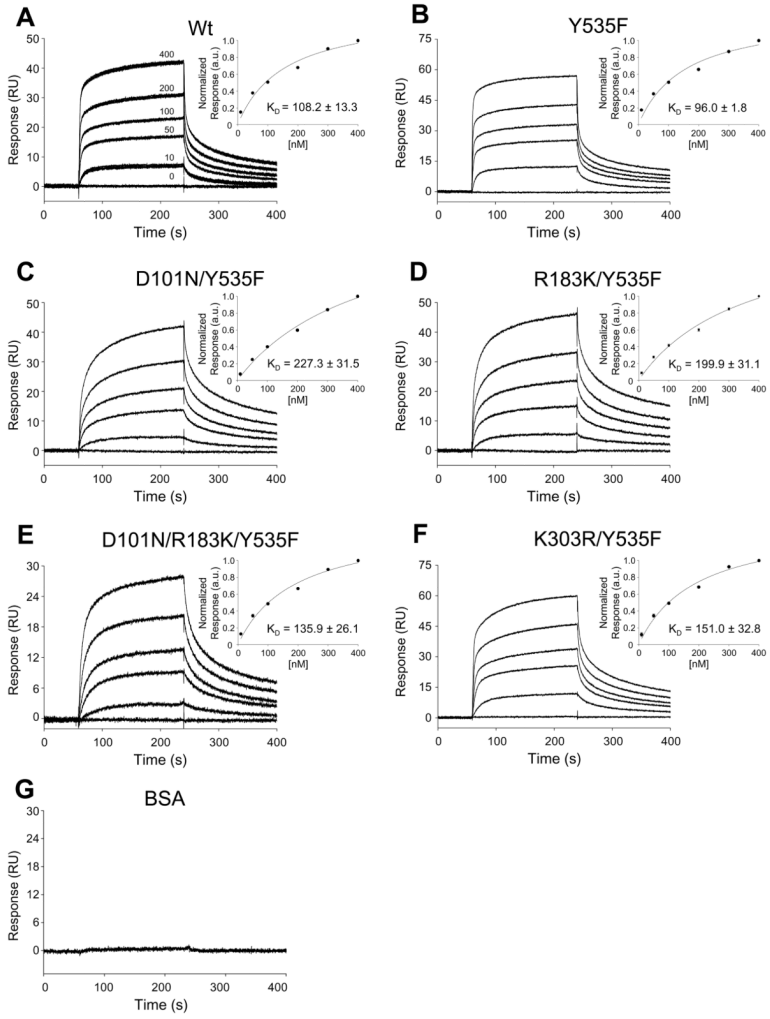

Figure 5. Binding of n-Src and NR2A C-tail proteins

SPR sensorgrams in A–F show the binding of wild-type and mutant n-Src proteins at concentrations of 0 to 400 nM to NR2A C-tail protein immobilized on a CM5 chip to a surface density of 2000 RU. Sensorgrams in panel A are displayed as overlaid triplicate experiments, while panels B–G are displayed as single representative experiments for clarity. The degree of reproducibility of the respective B–G triplicate runs was similar to that shown in panel A. G: SPR sensorgram showing the binding of BSA at 400 nM (negative control). Insets in A–F: Summary data showing affinity curves fit to a one-site binding model derived from SPR binding curves normalized to the response at 400 nM (mean ± SEM for each concentration of n-Src protein); K_D: (mean ± SEM) of steady-state binding constants (n = 6).

Table 1

n-Src constructs

n-Src Constructs	Corresponding c-Src Mutation	Mutation Location	Phenotype
Wild-type	None	None	Native
Y535F	Y527F	C-tail	Constitutively active
K303R/Y535F	K297R/Y527F	Kinase domain and C-tail	Kinase dead
D101N/Y535F	D99N/Y527F	SH3 domain and C-tail	SH3 domain dysfunction
R183K/Y535F	R175K/Y527F	SH2 domain and C-tail	SH2 domain dysfunction
D101N/R183K/Y535F	D99N/R175K/Y527F	SH3, SH2 domain and C-tail	SH3 and SH2 domain dysfunction
$Y535F^{\Delta 1–258}$	$Y527F^{\Delta 1–250}$	N-terminal, SH3, SH2 domain and C-tail	Deletion of N-terminal, SH3 and SH2 domain of active n-Src
K303R/$Y535F^{\Delta 1–258}$	K297R/$Y527F^{\Delta 1–250}$	N-terminal, SH3, SH2, kinase domain and C-tail	Deletion of N-terminal, SH3 and SH2 domain of kinase dead n-Src

The n-Src constructs are listed by the residue(s) mutated, corresponding mutation(s) in chicken c-Src, and respective phenotype based on the mutation(s).